Proceedings World Geothermal Congress 2000
Kyushu - Tohoku, Japan, May 28 - June 10, 2000

REFLECTION IMAGING OF HDR RESERVOIR AT SOULTZ BY MEANS OF THE AE REFLECTION METHOD

Nobukazu Soma[1)], Hiroaki Niitsuma[1)] and Roy Baria[2)]
[1)]Graduate School of Engineering Tohoku University, Sendai 980-8579, Japan
[2)]SOCOMINE, Rte de Kutzenhausen - B.P.39, F67250 Soultz-sous-Forêts, France

Key Words: geophysical prospecting, acoustic emission, reflection, hodogram, Soultz Hot Dry Rock site

ABSTRACT

This paper presents the reflection image of the Soultz Hot Dry Rock (HDR) reservoir by applying a type of reflection techniq ue which we call the AE reflection method where we use induced micro seismicity (acoustic emission: AE) as a wave source. We initially process the data to image some deep reflectors three dimensionally. Then we precisely relate these reflectors along the trajectory of the well GPK1, and obtained good agreement with other borehole observations. We have a lso analyzed along the expected well trajectory of deepened GPK2 before the actual drilling has finished in 1999. This results indicate a possible existence of some structures below pre-existing artificial reservoir, and are in harmony with estimates from microscopic examination of cuttings.

1. INTRODUCTION

Measurement around and below an existing reservoir is getting more important, because expansion of the developed area is one of the effective way to gain much more geothermal energy, including Hot Dry Rock (HDR) development for future energy resource. We, however, have no suitable technique to investig ate around or below the geothermal reservoir, because of the s pecific character of the geothermal area. For example, high te mperature and pressure prevent from using a conventional refl ection technique.

Therefore, we have developed a type of reflection technique called the AE reflection method where natural/induced seismicity are used as a seismic source (Soma and Niitsuma; 1997, Soma et al., 1997). The method was initially developed in time domain by using hodogram analysis, and we have already applied the method to some geothermal/HDR fields. The results indicated some reflectors in these field although it has not so high resolution.

Recently, we have modified the method to the time-frequency domain by applying the wavelet transform in order to get much higher resolution and reliability. The results indicates a great possibility to compare the estimate of the AE reflection method with other independent information and to characterize each reflector (Soma, 1998).

The European Hot Dry Rock programme has been successfully carried out at Soultz-sous-Forêt, north-east part of France, supported by EC, France, Germany and other organizations. The artificial heat exchanger was created around the depth from 2.0 to 3.5 km. The 4-month circulation test between well GPK1 and GPK2 was conducted in 1997 without water loss partly owing to use of a downhole pump (Baumgärtner et al., 1998). The well GPK2 was deepened toward 5km depth from February to May in 1999 for the purpose of development of scientific pilot plant. Now, it is possible to gather more information from the deeper region and to verify the results of the AE reflection method.

In this paper, we present the reflection image of the deep structure at the Soultz site and make a comparison with other borehole observations including data from the recently deepen ed GPK2. First, we will briefly describe about the AE reflecti on method in the time-frequency domain. Next, we shall describe the Soultz site and data sets used for the analysis. Then, we estimate the deep structure in the Soultz site and compare and discuss with other borehole information.

2. OUTLINE OF THE AE REFLECTION METHOD IN TIME-FREQUENCY DOMAIN

We can not detect reflected waves from raw observed waveform directly as they are covered by complex coda; randomly scattered waves. Therefore, we proposed a method to detect the reflected waves by examining the shape of three-dimensional hodogram which is a trace of the particle motion associated with the wave arrivals. It is known that the shape of the hodogram changes corresponding to the wave condition (Nagano et al., 1986). The shape of the hodogram is spherical for incoherent signal such as randomly scattered waves. However, it changes linearly when coherent signals such as direct P- and S-waves are detected. Therefore, we can detect reflected waves by analyzi ng the linearity of the hodogram under the assumption that ref lected waves are coherent signals.

For the evaluation of the shape of the hodogram in the time-fr equency domain, we evaluate a covariance matrix method by using the wavelet transform. The continuous-time wavelet transform of a function *s(t)* is:

$$W(b,a)=\int s(t')\,\frac{1}{\sqrt{a}}h^{*}\left(\frac{t'-b}{a}\right)dt' \qquad (1),$$

where *W(b, a)* is a wavelet coefficient,
h(t) is a window function used as an integral kernel called the analyzing wavelet, * means conjugate complex,
a is known as the scale factor called “scale” which represents the frequency component,
b is a translation factor of time called “shift”.

Here we use Mayer's orthogonal analyzing wavelet as *h(t)* because it can allow us to discuss a relationship of energy among multi-component wavelet coefficient.

We define a covariance matrix of the hodogram in time-frequ ency (Shift-Scale) domain, $S_{WT}(b, a)$, (equation (2)), since the wavelet transform can be regarded as a time-frequency distribution similar to a short-time Fourier transform (STFT).

$$S_{WT}(b,a)=\begin{pmatrix} W_{xx}(b,a) & W_{xy}(b,a) & W_{xz}(b,a) \\ W_{yx}(b,a) & W_{yy}(b,a) & W_{yz}(b,a) \\ W_{zx}(b,a) & W_{zy}(b,a) & W_{zz}(b,a) \end{pmatrix} \quad (2),$$

where $W_{ij}(b, a)=W_i(b, a)W_j^*(b, a)$
(* is conjugate complex), a: scale, b: shift, and
$W_i(b, a)$:wavelet coefficient of i component.

Samson's global polarization coefficient, *Cp(b, a),* (Samson, 1977) is shown in time-frequency domain:

$$Cp(b,a)=\frac{(\lambda_1-\lambda_2)^2+(\lambda_2-\lambda_3)^2+(\lambda_3-\lambda_1)^2}{2(\lambda_1+\lambda_2+\lambda_3)^2} \quad (3)$$

where $\lambda_i=\lambda_i(b,a)$: eigenvalues of the matrix (2)
for each time (shift: b) and frequency (scale: a)

By this parameter, we can quantitatively evaluate the shape of the hodogram in time-frequency domain; $Cp(b, a)$=1 at an ex act linear hodogram and $Cp(b, a)$=0 at a spherical hodogram. The coherent wave arrivals should have a high Cp value.

For the imaging of the subsurface structure, we have established a three-dimensional inversion of the waveform which shows the change of linearity in the hodogram. In this study, we focus on only simple S- to S-wave reflections because the energy of S-wave is more dominant in our application. We assume that P-wave reflection may be concealed by the energy of S-wave. The concept of the inversion is shown in Figure 1. This method is a type of diffraction stack migration. [1] The linearity waveform (formula (3)) of three-dimensional hodogram is used. [2] We can assume the iso-delay ellipsoid for a delayΔT. considering the detector, source, and path length. The virtual reflect points are located on the ellipsoid [3] The strength of the linearity waveform is plotted on the ellipsoid for all of the delay. Results are stacked for all events used in the analysis. Furthermore, we enhanced the resolution by a restriction of the virtual reflected points by examining the orthogonality between propagation direction and S-wave polarization. In addition, the effect of heterogeneous source distribution is compensated b y a normalization of wave density for a number of nearby eve nts for each source.

By the multi-component signal processing mentioned above, we can extract subsurface image in high resolution with the wavelet transform.

3. SOULTZ HDR TEST SITE AND DATA SETS

The Soultz HDR site is located in the north east of France, Alsace, on the western edge of the Rhine Graben, and has been developed since 1987 [Figure 2].

The geology of the site consists of shallow sedimentary layers and a deep granite below the depth of about 1400 m. There are a number of hydrothermal fractured zones in the granite. The two principle joint sets were detected striking N10E and N170E, dipping 65W and 70E, respectively (Baria et al., 1995). During 1992 - 1993, the well GPK1 was extended to 3590 m depth, a massive hydraulic injection was conducted, and an artificial heat exchanger was created in 1993. The second deep borehole, GPK2, was drilled in the periphery of the developed heat exchanger in early 1995 to a depth of 3876 m (Baumgärt ner et al., 1996). Then GPK2 was stimulated to improve the c onnection using brine and fresh water. During 1993 - 1996, a great number of microseismic events (AE events) were obs erved at several downhole detectors.

For the future industrial deployment of the HDR technology, it is necessary for the project to be extended towards higher flows and temperatures. Therefore, the geothermal well GPK2 was deepened toward 5km in 1999, providing additional information of the deep region along the well.

The AE data set we used for the analysis was observed during massive hydraulic experiment in 1993, because of the high quality. We selected 101 high energy events at observation well E4550, and those events were recorded with a length of 3 seconds longer than usual. The other observation wells were not suitable for the analysis because these particle motion were poorly recorded. Figure 3 shows the location of events for the analysis in 1993, observation point E4550, and orientations of estimated cross sections in the next section, Figure 4.

4. GENERAL DEEP REFLECTION STRUCTURE AT THE SOULTZ SITE

Figure 4 shows the estimate of the E-W and N-S cross sections by the AE reflection method in the time-frequency domain. These figures are estimates in (a) E-W section at 400 m north from the wellhead of GPK1, (b) E-W section at 400 m south, (c) N-S section at 100 m west, and (d) N-S section at 300 m east. We found several reflectors at depths of 3500 m, 3950 m, 4200 m, 4500 m, 4800 m and 5200 m.

We suppose that the reflectors around the depths of 3950 m o r 4200 m show a bottom of the artificial geothermal reservoir, since the fracture conditions may change there. The reflector around 3500 m depth may indicate one of the main permeable zones which were created during hydraulic fracturing in 1993. It is recognized that it is not possible to distinguish the reflector of weathered permeable zone from that of artificial created permeable zone.

However, for further interpretations, it is necessary to compare carefully the detected reflectors with other independent information. The GPK2 deepening in 1999 allows us to gather more information on deeper reflectors.

5. ESTIMATES ALONG DEEP WELLS AND COMPARISON WITH OTHER INFORMATION

We calculated the AE reflection method only along the well GPK1 using the same event sets as before. The resolution of the depth and the frequency range in the calculation are 2 m and 40 - 317 Hz, respectively.

The estimates along the GPK1 are shown in Figure 5. This figure shows the estimate by the AE reflection method (hodogram linearity which shows reflectivity in the method), number of fractures based on FMI log, density log, acoustic impedance log, thermal flow meter log, and helium log.

From the AE reflection method, we observe major peaks at the depths of 3100 m, 3200 m, 3330 m, 3375 m, 3500 m, and 3520 m. These estimates agree with number of fractures for depths below 3000 m. Changes in the density log and acoustic impedance log correspond to the peaks in the AE reflection method. The correspondence may be used to infer that the AE reflection method detects the fractures. The thermal flow meter log and helium log are one of the indicators of permeable fracture. Major permeable zones were reported in GPK1 around the depths of 2815 - 2817 m, 3192 - 3293 m, 3370 - 3406 m, and 3489 - 3496 m (Baria et al., 1994). Three major permeable zones can be detected from the AE reflection, exc ept for the one at a depth from 2815 - 2817 m.

We have estimated reflectors using the AE reflection method near GPK2 trajectory to a depth of 5000 m before the actual drilling started. Figure 6 shows the estimate of possible reflectors along the deep GPK2 (hodogram linearity). Here, we assumed a vertical well trajectory from the previous bottom of GPK2 to a depth of 5000 m, although the actual well is somewhat inclined. We found major peaks at the depths of 3850 m, 4000 m, 4100 m, 4425 m, 4650 m, 4750 m, 4850 m, and 4900 m. During the deepening GPK2, a synthetic petrog raphic log from microscopic examination of cuttings has bee n done and estimated the deep geological condition (Genter e t al., 1999). Figure 7 shows a geologic column estimated fro m cuttings. The existence of many fracture zones is postulate d, especially major fracture zones, composed of very highly a ltered granite, around a depth of 4575 m and 4775 m. These are may be one of the most permeable zones.

We should accept between 100 and 200 m difference in the comparison between Figure 6 and 7 because displayed trajectories of well are not the same. The peaks in the AE reflection method at the depths of 4425 m and 4650 m do correspond to two highly altered fracture zones at 4575 m and 4775 m depths. The other peaks may also correspond to some smaller fracture zones. Estimates from the AE reflection method along the deepened GPK2 have shown satisfactory agreement with geological estimates.

Comparison of the results of the AE reflection method with other data from boreholes has shown the detectability of fracture or altered zones. Detection from normal P-wave amplitude analysis is more difficult.

6. CONCLUSION

We have applied the AE reflection method in the time-freque ncy domain to the Soultz Hot Dry Rock site, France, and compared the reflection images with several borehole data in and below the depth of artificial geothermal reservoir. The results suggest that the method is useful to gather information on the existence of fracture or altered zones.

At the depth of the artificial reservoir in GPK1, the estimated structure agrees very well with the density of fractures. Some of permeable zones reported in GPK1 are also detected. There is, however, no significant difference in the observed results from permeable and non-permeable structure.

We have also estimated the structure along the expected well trajectory of the deepened well GPK2, before the drilling was finished. Some major likely reflectors were detected at the depths of 3850 m, 4000 m, 4100 m, 4425 m, 4650 m, 4750 m, 4850 m, and 4900 m. These results correspond well to a synthetic petrographic log from microscopic examination of cuttings, although there are acceptable differences in depth of the well trajectory.

We suppose that AE reflection method can detect a thin fractured structure. The technique shows that the method has a great potential as a useful tool for practical geothermal/HDR development in future, particularly from use of this method for deepening GPK2 in 1999. Our next target is the characterization of structures with the AE reflection method.

ACKNOWLEDGMENTS

This work was carried out as a part of MTC project and MURPHY project, both are supported by the New Energy and industrial technology Development Organization (NEDO), Japan (International Joint Research Grant). The work was also supported by the Japan Society for the Promotion of Science

(Grant JSPS-RFTF 97P00901). Authors also like to thank SOCOMINE for providing the data from European Hot Dry Rock site at Soultz-sous-Forêts. The European programme is supported by the EC, France, Germany, other funding and private agencies.

REFERENCES

Baria, R., Baumgärtner, J., Gérard, A. and Jung, R. (1994) *Scientific results associated with large scale hydraulic injection tests (a summary of the scientific programme carried out in 1993; 11/1/94).* The European Geothermal Energy Project at Soultz-sous-Forêts, Socomine Internal report.

Baria, R., Garnish, J., Baumgärtner, J., Gérard, A. and Jung, R. (1995) Recent Developments in the European HDR Research Programme at Soultz-sous-Forêts (France). *Proceedings of the World Geothermal Congress, 1995, Florence, Italy, International Geothermal Association,* vol.4, pp.2631-2637, ISBN 0-473-03123-X.

Baumgärtner, J., Jung, R. Gérard, A., Baria, R. and Garnish, J. (1996) The European HDR Project at Soultz-sous-Forêts: Stimulation of the Second Deep Well and First Circulation Experiments. *Proceedings 21st. Workshop Geothermal Reservoir Engineering, Stanford University,* Stanford, California, SGP-TR-151, pp.267-274.

Baumgärtner, J., Gérard, A., Baria, R., Jung, R., Tran-Viet, T., Gandy, T., Aquilina, L. and Garnish, J. (1998) Circulating the HDR Reservoir at Soultz: Maintaining Production and Injection Flow in Complete Balance - initial results of the 1997 circulation experiment. *Proceedings 23rd. Workshop Geothermal Reservoir Engineering, Stanford University,* Stanford, California, SGP-TR-158.

Genter, A., Homeier, G., Chevremont, Ph., Tenzer, H. (1999) *Deepening of GPK-2 HDR borehole, 3880-5090 m, (Soultz-sous-Forêts, France).* Geological monitoring. BRGM Open File Report, R 40685, 40 pp.

Nagano, K., Niitsuma, H. and Chubachi, N. (1986) A new automatic AE source location algorithm for downhole triaxial AE measurement, In: *Progress in acoustic emission III* Yamaguchi, K., et al (Ed.), The Japanese Soc. for NDI, pp.396-406.

Samson, J. C. (1977) Matrix and Stokes velocity representations of detectors for polarized waveforms: Theory, with some applications to teleseismic waves. *Geophys. J. Roy. Abstr. Soc.,* vol.51, pp.583-603.

Soma, N. and Niitsuma, H. (1997) Identification of structures within the deep geothermal reservoir of the Kakkonda field, Japan, by a reflection method using acoustic emission as a wave source, *Geothermics,* vol.26(1), pp.43-64.

Soma, N., Niitsuma, H., and Baria, R. (1997) Estimation of deeper structure at the Soultz Hot Dry Rock field by means of reflection method using 3C AE as wave source, *Pure and Applied Geophysics,* vol.150, pp.661-676.

Soma, N. (1998) Evaluation of deep geothermal reservoir structure by means of a reflection method using acoustic emission *Doctor thesis*, Graduate School of Tohoku University. (in Japanese)

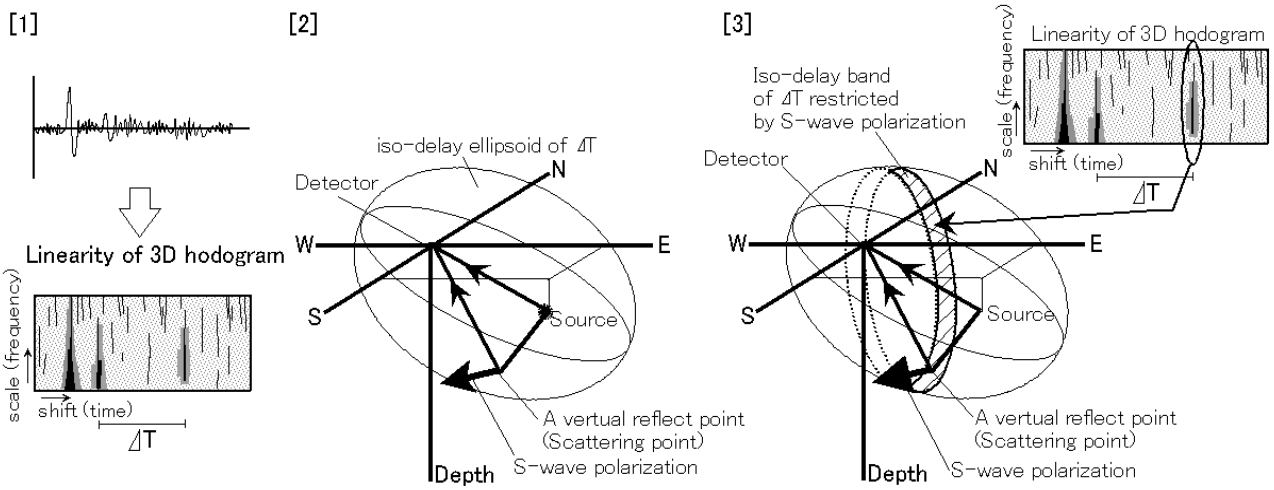

Figure 1. Concept of three-dimensional inversion by using the Wavelet transform

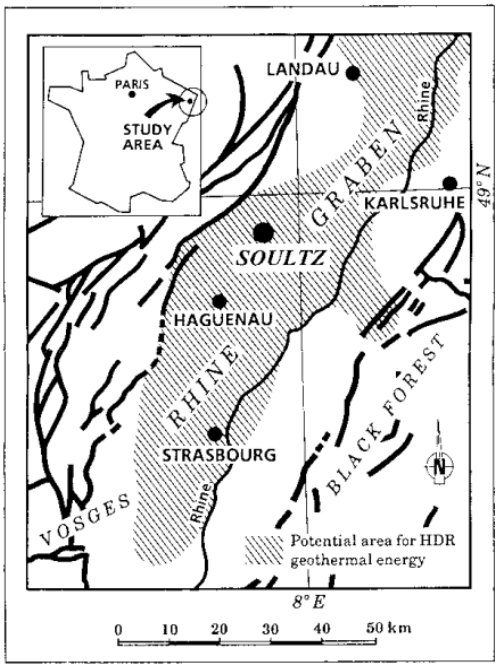

Figure 2. Location map of the Soultz-sous-Forêts site (France)

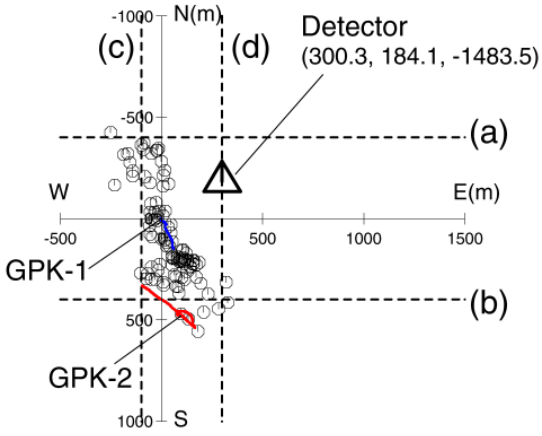

Figure 3. Horizontal location of 101 AE used in the analysis and orientation of estimated cross section in Figure 4 (a)-(d). Triangle shows observation well E4550.

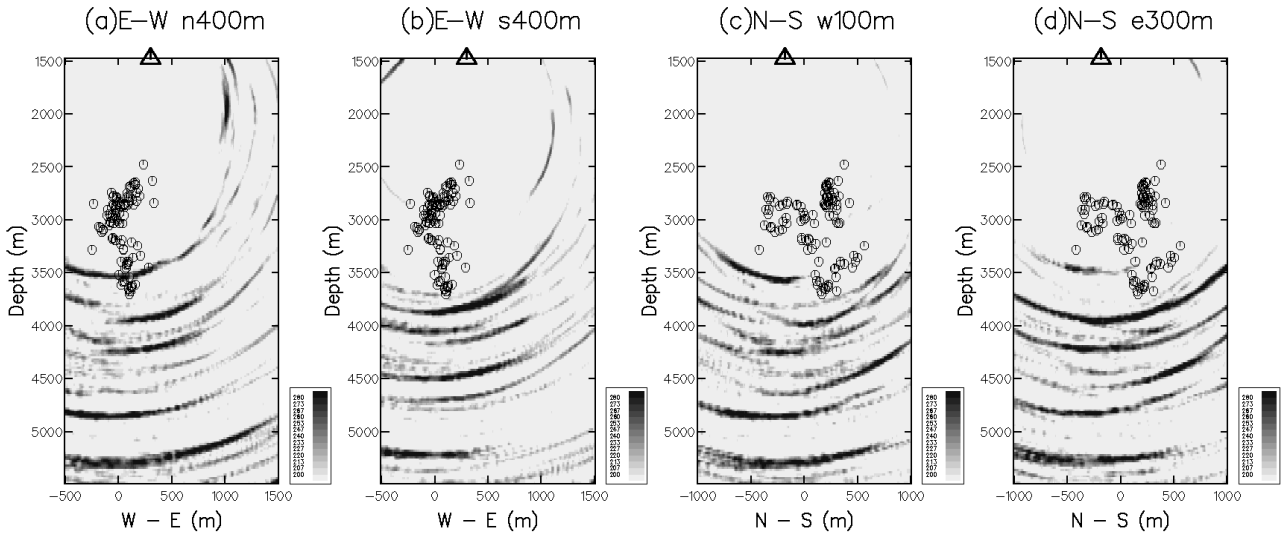

Figure 4. Deep estimation by the AE reflection method. (a):E-W cross section at 400 m north from well head of GPK1, (b):E-W cross section at 400 m south, (c):N-S cross section at 100 m west, (d):N-S cross section at 300 m east.

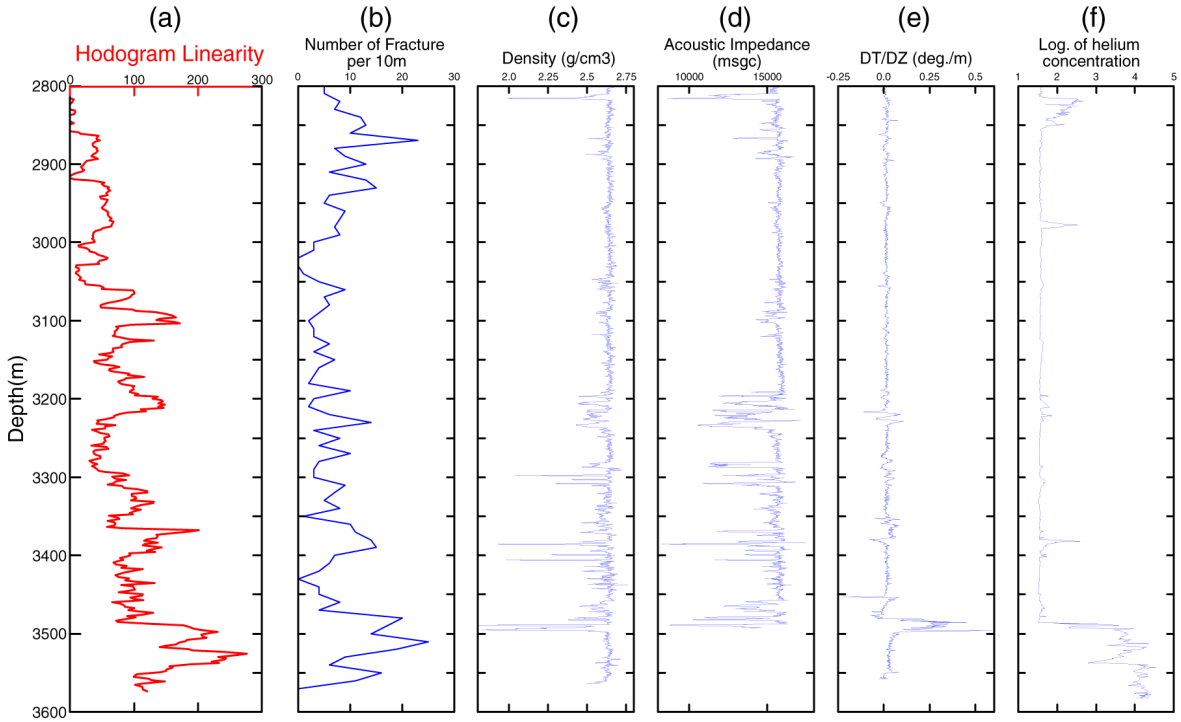

Figure 5. Estimation by the AE reflection method and several borehole observations ((a):Hodogram linearity from the AE reflection me thod, (b):Fracture density based on FMI log, (c):density log, (d):sonic log, (e):thermal flow meter log and (f):helium log) along GPK1.

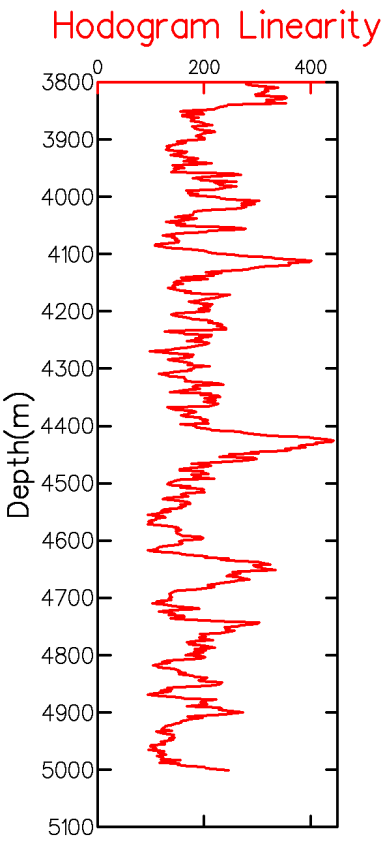

Figure 6. Estimation by the AE reflection method along deep GPK2.

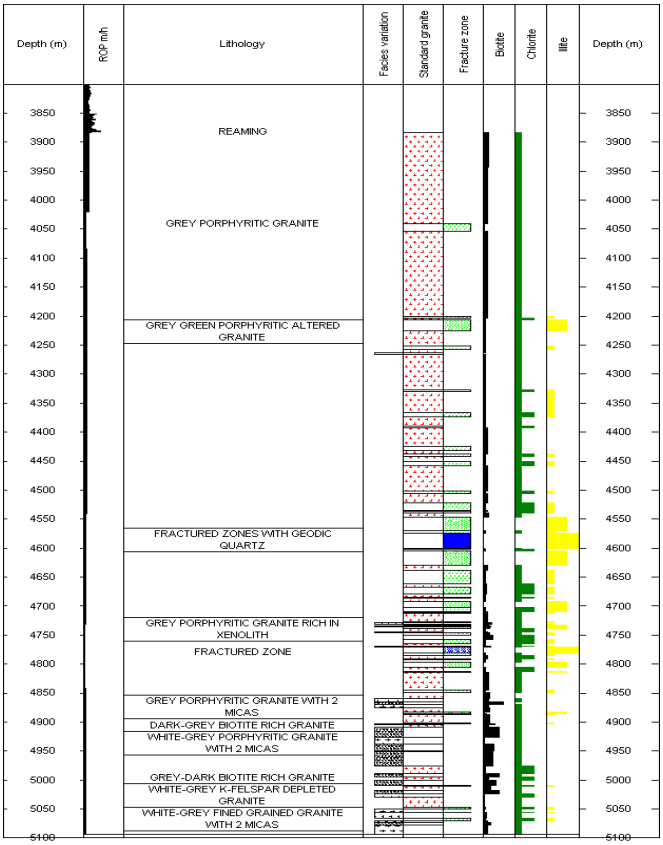

Figure 7. Result of synthetic petrographic log of GPK2 from microscopic examination of cuttings (Genter et al., 1999).